Received: 8 October 2022 | Accepted: 7 November 2022

DOI: 10.1002/pamm.202200256

# A phase field model for fractures in ice shelves

**Rabea Sondershaus**[1,*], **Angelika Humbert**[2,3], and **Ralf Müller**[1]

[1] Institut für Mechanik, Technische Universität Darmstadt, Franziska-Braun-Straße 7, 64287 Darmstadt, Germany
[2] Alfred-Wegener-Institut, Helmholtz Zentrum für Polar- und Meeresforschung, Bremerhaven, Germany
[3] University of Bremen, Department of Geosciences, Bremen, Germany

Ice shelves are large floating ice masses, that are formed when glaciers are becoming afloat at the margin of ice sheets. One dominating mass loss mechanism of ice shelves is calving, describing the detachment of icebergs at the front. Ice shelves stabilize inland ice glaciers due to buttressing. If the stabilizing effect of an ice shelf vanishes because of disintegration or thinning, the corresponding glacier accelerates resulting in sea level rise.

To describe calving and disintegration of ice shelves, it is important to investigate fracture propagation in ice. A powerful method in fracture mechanics is the phase field method which is based on Griffith's theory. It approximates cracks in a diffuse manner by using a continuous scalar field. We propose a phase field fracture model for ice considering its characteristic material properties. The material behavior of ice depends on the considered time scales. On short time scales it behaves like a solid and while it acts like a fluid on long time scales, which classifies it as a viscoelastic material of Maxwell type. This has been verified by observations. The phase field method allows us to simulate typical fracture situations of ice shelves in Antarctica and Greenland.



## 1 Introduction

Calving of icebergs from floating ice masses and tidewater glaciers is an important, but poorly understood process of ice sheets. Calving laws, describing this process are often simple empirical relations which are tuned by observational data [1], as the process in itself is of complex nature and a physical calving law has not yet been found. This has major implications for projections of ice sheets, which require an adequate representation of calving for simulating the evolution of the lateral margins of ice sheets reasonably well. Therefore detailed process-based models are needed, which allow to simulate the formation and propagation of cracks in ice.

In the last decades the phase field method has been established in fracture mechanics. In this method the physical discontinuity of a crack is represented by a continuous scalar field $s(x,t)$ which distinguishes between fully intact material, where $s=1$, and broken material $s=0$. The transition from one phase to another is controlled by a length scale $l_0$. Consequently the sharp crack interface $\Gamma$ is smoothed out, as sketched in Figure 1. The unified framework of the phase field method has the advantage that crack initiation, crack propagation and crack branching can all be modeled by the same method. In the last years different fracture mechanisms such as brittle [2–4], dynamic [5–7], fatigue [8–10] and hydraulic fracture [11, 12] were studied. Whereby latter was applied to the framework of glaciers recently [13]. Furthermore the method has been extended to anisotropic [14–16], plastic [17–19] and viscoelastic materials [20, 21]. All citations above are exemplary without claiming completeness.

This paper presents a variant of the phase field method suitable for fracture processes in ice, wherefore we adjust the energy potential to the special material behavior of ice. Furthermore first numerical results of a representative example are given.

## 2 Ice rheology

Ice is, viewed on a short time scale, an elastic material. In rheology elastic materials can be represented by a spring characterized by a Young's modulus $E$. The linear elastic stress $\sigma^e$ is calculated by $\sigma^e = E\varepsilon^e$. However on long time scales ice flows and therefore also shows viscous material behavior. Viscous materials can be represented by a dashpot with a viscosity $\eta$. The viscous stress $\sigma^v$ is proportional to the strain rate $\sigma^v = \eta\dot{\varepsilon}^v$. The combination of both leads to viscoelastic behavior. To derive a constitutive equation for this characteristic material behavior the spring and dashpot are connected in series, which leads to a Maxwell model as shown in Figure 2. The comparison between simulations and field observations verified that ice in glaciers indeed behaves like a Maxwell material [22]. The stresses acting on the spring $\sigma^e$ and on the damper $\sigma^v$ are equal to the total stress of the system $\sigma$ resulting in

$$\sigma = \sigma^e = E\varepsilon^e = \sigma^v = \eta\dot{\varepsilon}^v \,. \tag{1}$$

Whereas the overall strain $\varepsilon$ is the sum of the elastic strain $\varepsilon^e$ and the viscous strain $\varepsilon^v$

$$\varepsilon = \varepsilon^e + \varepsilon^v \,. \tag{2}$$

* Corresponding author: e-mail rabea.sondershaus@tu-darmstadt.de

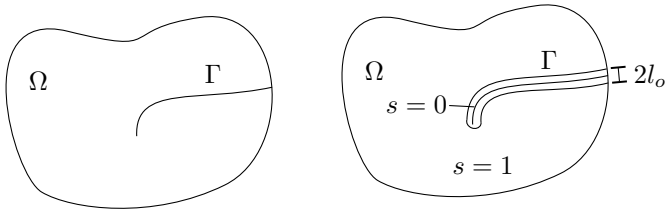


**Fig. 1:** A sharp crack interface $\Gamma$ within a domain $\Omega$ is shown on the left side, whereas the right panel shows the phase field representation of the same crack. The phase field variable $s$ thereby varies within the crack width $l_0$ between 1 for the fully intact material and 0 for the fully broken phase.

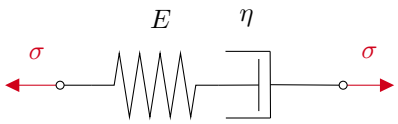


**Fig. 2:** Maxwell model: a spring and a dashpot are connected in series.

The viscous strain $\varepsilon^v$ can be interpreted as an internal variable. By combining (1) and (2) an evolution equation for this variable is derived as

$$\dot{\varepsilon}^v = \frac{E}{\eta}(\varepsilon - \varepsilon^v)\,. \tag{3}$$

And the constitutive equation for a Maxwell material is given by

$$\sigma = E(\varepsilon - \varepsilon^v)\,. \tag{4}$$

## 3 Phase field model for fracture

The energy potential for an elastic body in the phase field framework consists of two parts, the elastic strain energy $\psi^e$ and the fracture energy $\psi^f$. Following previous work on viscoelastic materials [20, 21] a term related to the viscous energy $\psi^v$ is added. This results in the following pseudo potential

$$\Pi \;=\; \int_\Omega \psi^e dV + \int_\Omega \psi^f dV + \int_\Omega \psi^v dV\,. \tag{5}$$

The elastic strain energy with a bulk modulus $K$ and a shear modulus $\mu$ can be additively decomposed into a volumetric $\psi^e_{vol}$ and deviatoric $\psi^e_{dev}$ part

$$\begin{aligned}\psi^e &= \quad \psi^e_{vol} \quad\quad +\psi^e_{dev}\\ &= \tfrac{1}{2}K\varepsilon^e_{vol}\varepsilon^e_{vol} \quad +\mu\boldsymbol{\varepsilon}^e_{dev} : \boldsymbol{\varepsilon}^e_{dev}\,,\end{aligned}$$

where $\varepsilon^e_{vol} = \mathrm{tr}(\boldsymbol{\varepsilon}^e)$ is the trace of the elastic strain tensor. The deviatoric part of the elastic strain is given by

$$\boldsymbol{\varepsilon}^e_{dev} = \boldsymbol{\varepsilon}^e - \frac{1}{3}\mathrm{tr}(\boldsymbol{\varepsilon}^e)\mathbb{1}\,.$$

The scalar product of two second order tensors is denoted by : and the second order identity tensor by $\mathbb{1}$.

The loss of stiffness in fractured material is modeled by the degradation function $g(s)$. A quadratic function $g(s) = s^2 + \eta_{RS}$ with a small residual stiffness $\eta_{RS}$ is used. The residual stiffness ensures numerical stability for the fully broken phase.

Different approaches exist to avoid crack formation under compression. Here we use Macaulay brackets

$$\langle x\rangle_+ = \begin{cases} x & x \geq 0 \\ 0 & x < 0 \end{cases} \quad \text{and} \quad \langle x\rangle_- = \begin{cases} x & x \leq 0 \\ 0 & x > 0 \end{cases}\,,$$

which split the volumetric strain energy into its positive and negative part. Finally the elastic strain energy is given by

$$\int_\Omega \psi^e dV \;=\; \int_\Omega g(s)\left(\frac{1}{2}K\langle\varepsilon^e_{vol}\varepsilon^e_{vol}\rangle_+ + \mu\boldsymbol{\varepsilon}^e_{dev} : \boldsymbol{\varepsilon}^e_{dev}\right) + \frac{1}{2}K\langle\varepsilon^e_{vol}\varepsilon^e_{vol}\rangle_- dV\,. \tag{6}$$

According to [23] the fracture energy needed to create new surfaces is modeled by

$$\psi^f = \mathcal{G}_c\left(\frac{(1-s)^2}{4l_o} + l_o\nabla s\cdot\nabla s\right)\,, \tag{7}$$

depending on the gradient of the phase variable $\nabla s$, the regularisation parameter $l_0$ and a material property $\mathcal{G}_c$, which is the critical energy release rate. In plane stress state it is connected to the critical fracture toughness $K_{Ic}$ from the classical concept

 

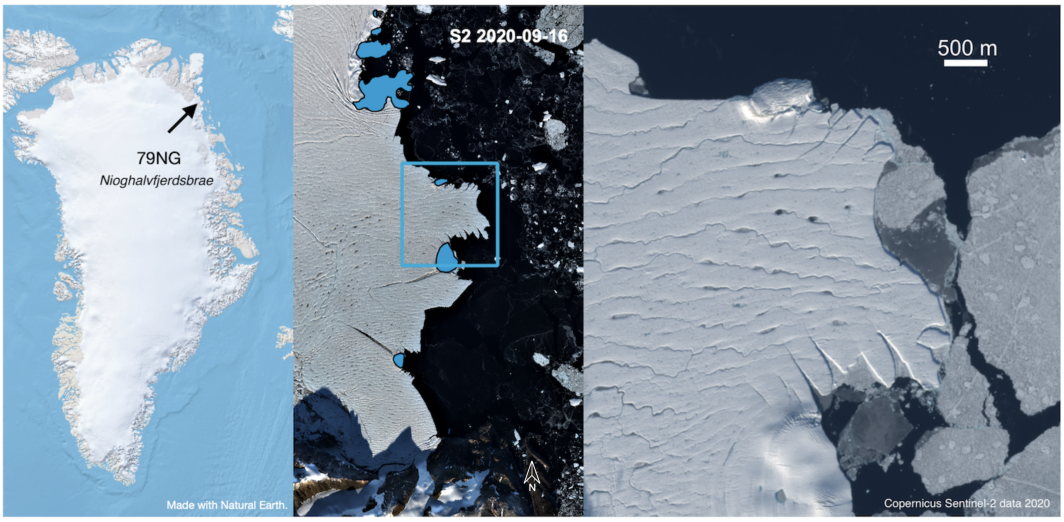


**Fig. 3:** The left panel displays a map of Greenland indicating the location of 79°N Glacier. The middle panel is a satellite image taken in September 2020 from the glaciers floating tounge and its calving front. The glacier flows from west to east. The pinning points are marked with light blue color. The right panel is a detail image showing the blue frame (Copernicus Sentinel-2 data 2020).

of stress intensity factors by $K_{Ic} = \sqrt{E\mathcal{G}_c}$. The critical fracture toughness in turn can be determined from experiments. The viscous contribution can be derived by Biot's equation [24] and is given by

$$\psi^v = \int_\Omega \int_t \frac{1}{2}\eta\dot{\boldsymbol{\varepsilon}}^v : \dot{\boldsymbol{\varepsilon}}^v dV \,. \tag{8}$$

It incorporates the viscous strain rate $\dot{\boldsymbol{\varepsilon}}^v$. Assuming that only the elastic energy drives the crack propagation the viscous energy is not degraded. This is in alignment with [22] which have shown that cracks exist in areas with high elastic strains at the 79°N Glacier in Greenland. To approximate the strain rate $\dot{\boldsymbol{\varepsilon}}^v$ a backwards Euler scheme

$$\dot{\boldsymbol{\varepsilon}}^v = \frac{\boldsymbol{\varepsilon}^v_{n+1} - \boldsymbol{\varepsilon}^v_n}{\Delta t} \,,$$

is used, leading to an incremental pseudo potential.

In total (6)-(8) result in

$$\begin{aligned} \Pi \;=\; & \int_\Omega g(s)\left(\frac{1}{2}K\langle\varepsilon^e_{vol}\varepsilon^e_{vol}\rangle_+ + \mu\boldsymbol{\varepsilon}^e_{dev} : \boldsymbol{\varepsilon}^e_{dev}\right) + \frac{1}{2}K\langle\varepsilon^e_{vol}\varepsilon^e_{vol}\rangle_- dV \\ & + \int_\Omega \mathcal{G}_c\left(\frac{(1-s)^2}{4l_o} + l_o\nabla s\cdot\nabla s\right)dV + \int_\Omega\int_t \frac{1}{2}\eta\dot{\boldsymbol{\varepsilon}}^v : \dot{\boldsymbol{\varepsilon}}^v dV \,. \end{aligned} \tag{9}$$

The solution of our problem is found by minimizing the pseudo functional (9). For this we set the variational derivative of the incremental pseudo potential $\delta\Pi$ to zero. The evolution equation of the phase field, that results from the variation of the potential with respect to $s$, is a Ginzburg-Landau equation $\dot{s} = -M\delta_s\Pi$ in which a mobility parameter is introduced to enhance the numerical stability of the system. The discretised system is solved using a monolithic scheme, that solves for all unknowns, i.e. the displacement $\vec{u}$, the phase field $s$ and the internal variable $\boldsymbol{\varepsilon}^v$, at the same time. Displacement $\vec{u}$ and total strain $\boldsymbol{\varepsilon}$ are related in the framework of infinitesimal strains by

$$\boldsymbol{\varepsilon} = \frac{1}{2}\left(\nabla\vec{u} + \nabla\vec{u}^T\right) \,.$$

The time steps were chosen adaptivly depending on the iterations needed by the Newton solver.

## 4 Numerical example

The phase field model is used to simulate the crack evolution in ice shelves at so called pinning points. Pinning points are where the normally floating ice shelf is grounded forming small ice caps. As can be seen in the satellite image form the 79°N Glacier shown in Figure 3 cracks arise at pining points denoted by the light blue areas. The ice flows from west to east into the ocean, appearing black in the image and the crack direction is perpendicular to the flow direction. Pinning points exist at several ice shelves, in particular in Antarctica and have a huge impact on the stability of ice sheets, because they buttress the inland ice and hence provide additional stability. However they are also responsible for the formation of cracks, leading to normal calving as shown in Figure 3.

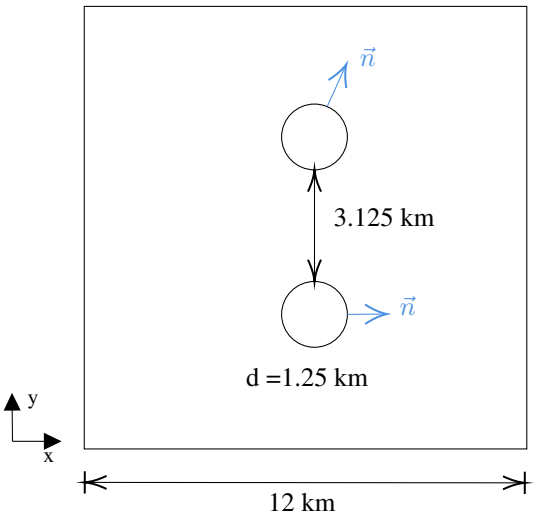


**Fig. 4:** Top view of the model domain.

**Table 1:** Material parameters for ice [25, 26].

| Quantity | Symbol | Value | Unit |
|---|---|---|---|
| Young's modulus | $E$ | $9 \cdot 10^9$ | Pa |
| Poisson's ratio | $\nu$ | 0.325 | |
| viscosity | $\eta$ | $9 \cdot 10^{14}$ | Pa s |
| fracture toughness | $K_I$ | $95 \cdot 10^3$ | $\mathrm{Pa\,m^{1/2}}$ |

Our model domain is a rectangular subset of the ice shelf with a length and width of $12\,\mathrm{km}$. The height is given by $1\,\mathrm{km}$. A top view of the model domain can be found in Figure 4. The coordinate system is defined such that the flow direction is along the x-axis. The pinning points are introduced by two spherical segments protruding $100\,\mathrm{m}$ into the ice shelf with a sphere ring diameter of $1250\,\mathrm{m}$ at the bottom of the ice shelf. The dimensions were determined to roughly fit the dimensions of 79°N Glacier.

The ice can flow around the spherical segments but not into them. To ensure this, a no penetration condition by means of a penalty term is added to the energy potential

$$\Pi + p \int_{\Gamma_{\mathrm{pp}}} \frac{1}{2} \left(\vec{u} \cdot \vec{n}\right)^2 \, dA = 0\,. \tag{10}$$

Thereby $\vec{n}$ is the outer normal vector of the sphere segments $\Gamma_{\mathrm{pp}}$ representing the pinning points, see Figure 4. The penalty parameter $p = 10 \cdot 10^{10}$ is chosen such that a sufficient compliance of the boundary condition is reached.

Fracture is an irreversible process but it is not a priori governed by the Ginzburg-Landau ansatz. Therefore an irreversible constraint of Dirichlet type is implemented to prevent crack healing. A constant horizontal velocity of $v_x = 2\,\mathrm{m\,day^{-1}}$ over the hole ice thickness is applied at the downstream side of the ice shelf leading to tension stress state of the domain. The material parameters used throughout the simulations are taken from [25, 26] and are specified in Table 1. The finite element framework *FEniCS* [27, 28] was used to implement and run the phase field model while the mesh was created with *Gmsh* [29].

### 4.1 Results

At the bottom of the ice shelf at each pinning point a crack begins to form. They propagate radially in the $y$-$z$-plane, which is perpendicular to the flow direction. The onset of the cracks can be seen in Figure 5 a) where the phase field variable under the threshold of $0.1$ is plotted in blue, so that the emerged cracks are visualized. After the onset, the cracks evolve no longer symmetrically around the pinning points but rather towards the middle of the domain. Thereby they reach the entire thickness of the ice shelf. Afterwards the two cracks unify in the area between the pinning points, see Figure 5 b). Then the unified crack propagates to the sides of the domain shown in Figure 5 c) until it is completely separated. In Figure 5 d) the state of the phase field at the end of the simulation is shown.

Comparing the results of the simulation to the satellite data, a good qualitative agreement can be found. In both cases the cracks occur at the pinning points and the crack paths are perpendicular to the flow direction. The phase field model is thus indeed a physical based model for crack initiation and propagation at calving fronts. As can be seen in Figure 3, the cracks occurring at the pinning points at 79°N Glacier arrest and move further downstream. This behavior is not captured in the numerical model so far due to the small strain theory. Instead the cracks in our simulation tear the entire area between the pinning points. Hence an extension to finite strain will improve the model.

## 5 Conclusion

We proposed a phase field model for fracture which incorporates the viscoelastic behavior of ice. Our simulations of the crack path match very well with the observed crack paths at 79°N Glacier. The phase field method for fracture is thus a promising approach to a physical calving model. Further investigations are needed to derive a better understanding of the viscous contribution of the Maxwell model to fracture processes. Furthermore the model should be extended to the framework

 

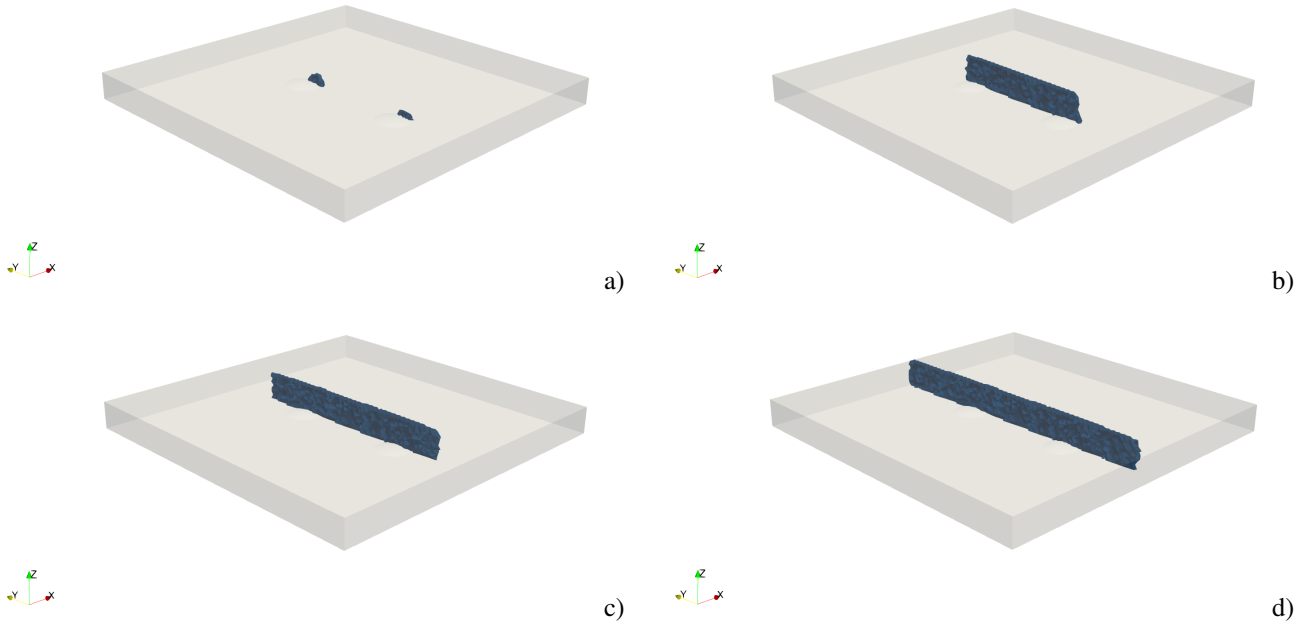


**Fig. 5:** Simulation results at different times: the model domain is plotted in grey whereas the result of the phase field for $s \leq 0.1$ is plotted in blue. The threshold is chosen arbitrarily such that the crack topology is well visible.

of large deformations and finite strains to be able to investigate longer time scales. Therefore a multiplicative split of the deformation gradient into a elastic and viscous part will be utilized within the context of the rheology of ice see [30]. In addition the flow behavior of polycrystalline ice is rate dependent [31] in a power law manner. This is described by Glen's flow law, which we also want to incorporate in further works.

**Acknowledgements** Support for this research was provided by the German Research Foundation (DFG) under grant number 501994052. The authors gratefully acknowledge the computing time provided on the high-performance computer Lichtenberg at the NHR Centers NHR4CES at TU Darmstadt. Open access funding enabled and organized by Projekt DEAL.

## References

[1] Benn, D. I., and Åström J. A. *Calving glaciers and ice shelves.* Advances in Physics: X, 3(1), pp. 1048–1076, 2018
[2] Francfort, G. A., and Marigo, J. J. *Revisiting brittle fracture as an enerty minimization problem.* Journal of the Mechanics and Physics of Solids, 46(8), pp. 1319–1342, 1998.
[3] Bourdin, B., Francfort, G. A., and Marigo, J. J. *Numerical experiments in revisited brittle fracture.* Journal of the Mechanics and Physics of Solids, 48(4), pp. 797–826, 2000.
[4] Bourdin, B. *Numerical implementation of the variational formulation for quasi-static brittle fracture.* Interfaces and Free Boundaries, 9(3), pp. 411–430, 2007.
[5] Borden, M. J., Verhoosel, C. V., Scott, M. A. Hughes, T. J., and Landis, C. M. *A phase-field description of dynamic brittle failure.* Computer Methods in Applied Mechanics and Engineering, 217, pp. 77–95, 2012.
[6] Schlüter, A., Kuhn, C., Müller, R., and Gross, D. *An investigation of intersonic fracture using a phase field model.* Archive of Applied Mechanics, 86, pp. 321–333, 2016.
[7] Ren, H. L., Zhuang, X. Y., Anitescu, C., and Rabczuk, T. *An explicit phase field method for brittle dynamic fracture.* Computers & Structures, 217, pp. 45–56, 2019.
[8] Lo, Y. S., Borden, M. J., Ravi-Chandar, K., and Landis, C. M. *A phase-field model for fatigue crack growth.* Journal of the Mechanics and Physics of Solids, 132, p. 103684, 2019.
[9] Schreiber, Ch., Kuhn, Ch., Müller, R., and Zohdi, T. *A phase field Modeling approach of cyclic fatigue crack growth.* International Journal of Fracture, 225, pp. 89–100, 2020.
[10] Yan, S., Schreiber, C., and Müller, R. *An efficient implementation of a phase field model for fatigue crack growth.* International Journal of Fracture, pp. 1–14, 2022.
[11] Heider, Y. *A review on phase-field modeling of hydraulic fracturing.* Engineering Fracture Mechanics, 253, pp. 1–24, 2021.
[12] Aldakheel, F., Noii, N., Wick, T. and Wriggers, P. *A global–local approach for hydraulic phase-field fracture in poroelastic media.* Computers & Mathematics with Applications, 91, pp. 99–121, 2021.
[13] Clayton, T., Duddu, R., Siegert, M. and Martínez-Pañeda, E. *A stress-based poro-damage phase field model for hydrofracturing of creeping glaciers and ice shelves.* Engineering Fracture Mechanics, 272, pp. 1–24, 2022.

[14] Teichtmeister, S., Kienle, D., Aldakheel, F., and Keip, M. A. *Phase field modeling of fracture in anisotropic brittle solids.* International Journal of Non-Linear Mechanics, 97, pp. 1–21, 2017.
[15] Bleyer, J. and Alessi, R. *Phase-field modeling of anisotropic brittle fracture including several damage mechanisms.* Computer Methods in Applied Mechanics and Engineering, 336, pp. 213–236, 2018.
[16] Schreiber, C. *Phase Field Modeling of Fracture: Fatigue and Anisotropic Fracture Resistance.* Ph.D. Thesis, TU Kaiserslautern, 2021.
[17] Ambati, M., Gerasimov, T., and De Lorenzis, L. *Phase-field modeling of ductile fracture.* Computational Mechanics, 55(5), pp. 1017–1040, 2015.
[18] Miehe, C., Aldakheel, F., and Raina, A. *Phase field modeling of ductile fracture at finite strains: A variational gradient-extended plasticity-damage theory.* International Journal of Plasticity, 84, pp. 1–32, 2016.
[19] Noll, T., Kuhn, Ch., Olesch, D., and Müller, R. *3D phase field simulations of ductile fracture.* GAMM Mitteilungen, 43, 2020.
[20] Shen, R., Waisman, H., and Guo, L. *Fracture of viscoelastic solids modeled with a modified phase field method.* Computer Methods in Applied Mechanics and Engineering, 346, pp. 862–890, 2019.
[21] Dammaß, F., Ambati, M., and Kästner, M., *A unified phase-field model of fracture in viscoelastic materials.* Continuum Mechanics and Thermodynamics, 1-23, 2021.
[22] Christmann, J., Helm, V., Khan, S. A.,Kleiner, T, Müller, R., Morlighem, M., Neckel, N., Rückamp, M., Steinhage, D., Zeising, O. and Humbert, A., *Elastic deformation plays a non-negligible role in Greenland's outlet glacier flow.*, Communications Earth & Environment 2(1), pp. 1–12 , 2021
[23] Ambrosio, L., and Tortorelli, V. M. *On the approximation of free discontinuity problems*, Boll. Un. Mat. Ital. B(7), pp. 105–123, 1992.
[24] Biot, M. A. *Mechanics of incremental deformations.* 1965.
[25] Christmann J., *Viscoelastic Modeling of Calving Processes at Antarctic Ice Shelves.* Ph.D. Thesis, TU Kaiserslautern, 2017.
[26] Christmann, J., Müller, R., Webber, K. G., Isaia, D., Schader, F. H., Kipfstuhl, S., Freitag, J., and Humbert, A. *Measurement of the fracture toughness of polycrystalline bubbly ice from an Antarctic ice core.* Earth System Science Data, 7(1), pp. 87–92, 2015.
[27] Alnaes, M. S., Blechta, J., Hake, J., Johansson, A., Kehlet, B., Logg, A., Richardson, C., Ring, J., Rognes, M. E. and Wells, G. N. *The FEniCS Project Version 1.5*, Archive of Numerical Software 3, 2015.
[28] Logg, A., Mardal, K.-A., Wells, G. N., et al, *Automated Solution of Differential Equations by the Finite Element Method.* Springer, 2012.
[29] Geuzaine, C., and Remacle, J.-F. *Gmsh: a three-dimensional finite element mesh generator with built-in pre- and post-processing facilities.* International Journal for Numerical Methods in Engineering 79(11), pp. 1309-1331, 2009.
[30] Christmann, J., Müller, R. and Humbert, A., *On nonlinear strain theory for a viscoelastic material model and its implications for calving of ice shelves.* Journal of Glaciology 65(250), pp. 212–224, 2019.
[31] Glen, J. W. *The creep of polycrystalline ice.* Proceedings of the Royal Society of London, Series A, Mathematical and Physical Sciences, 228(1175), pp. 519–538, 1955.